A comparison of approximations for the converted-wave reflection

Maria Donati and Nicolas W. Martin

ABSTRACT

AVO analysis for converted waves has been restricted mainly to model AVO responses as a function of offset, varying some horizon characteristics, such as thickness and V_p/V_s ratio. To generalize, facilitate, and make comparable to P-P AVO analysis, the converted wave reflection coefficient, $R^{ps}(\theta)$, given by Aki and Richards (1980), has been simplified through different approaches. Each approximation has associated different levels of error, which depends on how the original terms in $R^{ps}(\theta)$ are manipulated.

The best approximation, named R_1^{ps}, is valid for incidence angles between 0 and 90 degrees, but some terms do not provide any additional information about the elastic properties. In contrast, R_5^{ps} approach shows an error lower than 10 percent, for incidence angles between 0 and 50 degrees, and resembles Shuey's P-P quadratic approach. In this case, R_5^{ps} shows a more suitable expression to be inverted for elastic parameters through least squares fit.

The R_5^{ps} approach will provide inverted elastic parameters sections, such as: (i) a rigidity relative contrast and (ii) a S-wave velocity reflectivity (Smith and Gidlow, 1987). These sections could be potentially used to discriminate and recognize possible gas/oil zones, in conjunction with P-P AVO analysis.

INTRODUCTION

The practical application of P-P AVO analysis, for detecting gas sands, consists in expressing P-wave seismic amplitude, $R^{pp}(\theta)$, as a linear or quadratic dependence with angle of incidence (Shuey, 1985). From this linear approach two seismic sections are obtained: (1) a normal incidence section and (2) a gradient section related to lithologic changes in subsurface.

Only the gradient section provides information about Poisson's ratio contrast (Koefoed, 1955, 1962; Shuey, 1985). This elastic parameter represents the "lithologic" component because of a change in lithology is usually associated with a change in Poisson's ratio.

In contrast, P-S AVO analysis is still being developed for extracting elastic properties from multicomponent data. P-S AVO analysis has been mainly limited to model P-S AVO response vs offset (or incidence angle), $R^{ps}(\theta)$, varying the thickness and V_p/V_s ratio of the target horizon, for selecting offset ranges where P-S AVO response gives better information than P-P AVO response (Nazar, 1991; Donati, 1997).

Contents

Recently, Xu and Bancroft (1997) have shown several linear approximation of the P-S wave reflection coefficient which are valid for incidence angles lower than 30 degrees, as compared to Aki and Richards (1980) approach. This P-S AVO analysis can be applied to find density and rigidity relative contrasts under assumption of constant V_p/V_s ratio. Gulati and Stewart (1997) showed that $R^{ps}(\theta)$ can be expressed as a series of sine functions of P-wave incidence angle, which fits the Aki-Richards approximation very well for angles less than 60 degrees.

The present paper shows different P-S AVO approaches oriented to obtain elastic parameters from P-S data. Each approach has associated a different level of error with increasing incidence angle, which depends on how the original terms representing $R^{ps}(\theta)$ are manipulated, as established by Aki and Richards (1980). After inverting the P-S AVO response, by applying least squares fit, it will be possible to obtain information about rigidity relative contrast and S-wave velocity reflectivity (Smith and Gidlow, 1986), both related to presence of fluids. Integrating these should allow better lithologic characterization.

WHY INVERT ELASTIC PARAMETERS FROM P-S AVO RESPONSE?

The P-S reflection amplitude approximation, $R^{ps}(\theta)$, given by Aki and Richards (1980), assumes small changes in elastic properties through an interface. It can expressed as

$$R^{ps}(\theta) = \tag{1}$$

$$A\left[\left(1-2\frac{V_s^{\,2}}{V_p^{\,2}}\sin^2\theta+2\frac{V_s}{V_p}\cos\theta\cos\psi\right)\frac{\Delta\rho}{\rho}-\left(4\frac{V_s^{\,2}}{V_p^{\,2}}\sin^2\theta-4\frac{V_s}{V_p}\cos\theta\cos\psi\right)\frac{\Delta V_s}{V_s}\right]$$

where the normalization factor A is defined as

$$A=-\frac{V_p\tan\psi}{2V_s} \tag{2}$$

Figure 1 shows a comparison between P-S AVO and P-P AVO responses as a function of offset, considering different saturant fluids. P-S AVO is more sensitive to Poisson's ratio variations than P-P AVO does, for incidence angles lower than 80 degrees. In particular, for incidence angles around 80 degrees, P-P AVO does not show significant differences in behavior between a sand saturated with water and gas. In contrast, P-S AVO responses for gas-sand and water-sand is quite different.

Additionally, P-S AVO is more sensitive to thickness changes than P-P AVO, as observed on porous glauconitic sands (Nazar, 1990; Donati, 1997). This indicates that it will be very valuable to get elastic properties from P-S AVO analysis, because of these inverted properties could provide additional information about lithology and type of fluid, at middle and large offsets.

The principal problem of using Aki and Richards P-S approach is that its terms are coupled, making the task of inverting elastic properties very complicated. Then, it is

Contents

necessary to get more practical P-S AVO approximations, which represent Aki and Richards P-S behavior well enough, while letting us to obtain elastic properties in an easy way, i.e. least squares fit, like Shuey's P-P analysis. The following section shows different approaches to R^{ps} depending how are manipulated the original terms in $R^{ps}(\theta)$

DERIVATIONS

Using the Snell's law

$$\sin\psi = \frac{V_s}{V_p}\sin\theta \tag{3}$$

then

$$\cos\psi \cong 1 - \frac{1}{2}\frac{V_s^{\,2}}{V_p^{\,2}}\sin^2\theta \tag{4}$$

where V_p is P-wave velocity, V_s is S-wave velocity, θ is P-wave incident angles and ψ is S-wave reflected angle. Substituting eq. (4) in eq. (1), R^{ps} can be reduced to

$$R_1^{\,ps}(\theta) \cong NF\left[\left(\frac{\Delta\rho}{\rho} - 2\frac{V_s^{\,2}}{V_p^{\,2}}\frac{\Delta\rho}{\rho} - 4\frac{V_s^{\,2}}{V_p^{\,2}}\frac{\Delta V_s}{V_s}\right) + \left(2\frac{V_s}{V_p} - \frac{V_s^{\,3}}{V_p^{\,3}}\right)\frac{\Delta\rho}{\rho} + \left(4\frac{V_s}{V_p} - 2\frac{V_s^{\,3}}{V_p^{\,3}}\right)\frac{\Delta V_s}{V_s}\right]\cos\theta + \left[2\frac{V_s^{\,2}}{V_p^{\,2}}\frac{\Delta\rho}{\rho} + 4\frac{V_s^{\,2}}{V_p^{\,2}}\frac{\Delta V_s}{V_s}\right]\cos^2\theta + \left[\frac{V_s^{\,3}}{V_p^{\,3}}\frac{\Delta\rho}{\rho} + 2\frac{V_s^{\,3}}{V_p^{\,3}}\frac{\Delta V_s}{V_s}\right]\cos^3\theta \tag{5}$$

or

$$R_1^{\,ps}(\theta) = NF\left[A_o\cos\theta + A_1\cos^2\theta + A_2\cos^3\theta\right] \tag{6}$$

Figure 2 shows a comparison between $R^{ps}(\theta)$ and Aki-Richards approaches as a function of incidence angle. If incidence angles lower than 30 degrees are considered, the normalization factor (NF) can be expressed as

$$NF \cong \frac{V_s}{V_p}\sin\theta + \frac{1}{2}\frac{V_s^{\,3}}{V_p^{\,3}}\sin^3\theta \approx -\frac{\sin\theta}{2} \tag{7}$$

where the term including $\sin^3(\theta)$ have been dropped because it is very small. This simplification generates an additional P-S reflection approach, R_2^{ps}, given by

Contents

$$R_2^{ps}(\theta) = -\frac{\sin\theta}{2}\left[A_o + A_1\cos\theta + A_2\cos^2\theta + A_3\cos^3\theta\right] \quad (8)$$

It is evident from Fig. 3 that, the normalization factor (NF) controls P-S AVO amplitude incidence angles higher than 50 degrees. Then, the normalization factor is the principal factor affecting P-S AVO behavior at far-offset range.

If the term including $\cos^3(\theta)$ is eliminated, $R_3^{ps}(\theta)$ approach is obtained

$$R_3^{ps}(\theta) = -\frac{\sin\theta}{2}\left[A_o + A_1\cos\theta + A_2\cos^2\theta\right] \quad (9)$$

Figure 4 shows that this high-order cosine truncation affects P-S AVO behavior at middle-offset range. But, at the far-offset range this effect is very similar to that obtained using a simplification of the normalization factor (NF) (eq. 8).

The error curves for $R_1^{ps}(\theta)$, $R_2^{ps}(\theta)$, and $R_3^{ps}(\theta)$ approaches as compared to Aki-Richards approximations are indicated in Fig. 5. $R_2^{ps}(\theta)$ shows highest relative error (20-30%) while $R_2^{ps}(\theta)$ shows lowest relative error (1-2 \%).

If we use the following cosines approximations:

$$\cos\theta \cong 1 - \frac{1}{2}\sin^2\theta \quad (10)$$

$$\cos^2\theta = 1 - \sin^2\theta \quad (11)$$

$$\cos^3\theta \cong 1 - \frac{3}{2}\sin^2\theta \quad (12)$$

Then R_4^{ps} and R_5^{ps} approaches are represented by

$$R_4^{ps}(\theta) = -\frac{B_o}{2}\sin\theta + \frac{1}{4}\left(B_1 - B_o\frac{V_s^2}{V_p^2}\right)\sin^3\theta \quad (13)$$

$$R_5^{ps}(\theta) = -\frac{B_o}{2}\sin\theta + \frac{1}{4}\left(B_1 - B_o\frac{V_s^2}{V_p^2}\right)\sin^3\theta - \frac{1}{8}\frac{V_s^2}{V_p^2}B_1\sin^5 \quad (14)$$

where B_0 and B_1 are given by

$$B_o = \left(1 - 2\frac{V_s}{V_p}\right)\frac{\Delta\rho}{\rho} + 4\frac{V_s}{V_p}\frac{\Delta V_s}{V_s} \quad (15)$$

and

Contents

$$B_1 = 2\frac{V_s}{V_p}\left(1+\frac{V_s^{\,2}}{V_p^{\,2}}+2\frac{V_s}{V_p}\right)\left[\frac{\Delta\rho}{\rho}+2\frac{\Delta V_s}{V_s}\right] \qquad (16)$$

DISCUSSION

The basis of the derivation of eq. (1) from the exact Zoeppritz equation is that the percentage change in elastic properties is small, i,e., $\Delta V_s/V_s$ and $\Delta\rho/\rho$ are small compared to unity. For the vast majority of exploration situations this is no problem.

The basic difference between eq. (1) and (5) is the philosophy of grouping terms. Equation (5) displays which combinations of elastic properties are effective in successive ranges of angle θ. Equation (1) is arranged to separate the effects of the two variables $\Delta\rho$ and ΔV_s. Equation (5) diagonalizes the relationship between elastic properties and $R^{ps}(\theta)$ in the sense that certain features are related to certain combinations of elastic properties without significant coupling between the variables.

The R_1^{ps} approach shows an excellent fit to Aki-Richards approach until 90 degrees of incidence angle (Fig. 2). The S reflected angle is explicitly eliminated from the P-S reflection coefficient, which does R_1^{ps} suitable to be obtained from conventional ray tracing modeling. However, it is still need to know the P-S offset which is considered as a function of the P-P offset. Additionally, some terms of R_1^{ps} approach do not provide any additional information about the elastic properties $\Delta V_p/V_p$ and $\Delta V_s/V_s$, i.e., A_2 and A_3 (eq. 5).

R_2^{ps} approach shows a good fit to Aki-Richards approach until 60 degrees of incidence angle (Fig. 3). The V_p/V_s ratio is eliminated from the "Normalization Factor" (A). The choice of factor A bias the inverted elastic properties $\Delta V_p/V_p$ and $\Delta V_s/V_{s,}$ when observed amplitudes are fitted at high angles. R_2^{ps} is easy manipulate foe elastic property estimation (Figs. 3,5).

R_3^{ps} approach represents a truncation of higher power of $\cos\theta$, but it affects the fit at middle angles (20 - 40 degrees). This fact generates or under-estimated elastic properties at middle angles. However, the general amplitude behavior is kept for P-S AVO qualitative analysis (Figs. 4,5).

Finally, the R_4^{ps} and R_5^{ps} approaches fit very well to Aki-Richards approximation for angles lower than 50 degrees. Both, R_4^{ps} and R_5^{ps} resemble P-P Shuey's approach valid for incidence angles lower than 30 degrees. The elastic parameters are easily obtained assuming a V_p/V_s ratio, through a least squares fit (Fig. 6).

The percent errors for each P-S AVO is shown in Fig. 5. It is evident that minimum errors are associated with R_1^{ps} and R_5^{ps}, (< 10%) while higher absolute errors are shown by R_3^{ps} (> 20%).

CONCLUSIONS

Through the linearization of the converted-wave reflection coefficient, we have the possibility of applying AVO analysis in a easy way and comparable to the P-wave

Contents

data. We have found that the best approximation for the reflection coefficient is given by R_5^{ps} which shows a more suitable expression to be inverted for elastic parameters through least-squares fit.

REFERENCES

Aki,K. and Richards, P.G., 1980, Quantitative seismology: Theory and methods, v. 1: W.H. Freeman and Co.

Donati, M.S., 1997, Synthetic example of the benefits of P-SV AVO analysis in the glauconitic channel-Blackfoot field, Alberta, 59th EAGE Meeting, Geneva, Extended Abstracts, 2, C014.

Koefoed, O., 1955, On the effect of Poisson's ratios of rock strata on the reflection coefficients of plane waves: Geophysical Prospecting, 3, 381-387.

Koefoed, O., 1962, Reflection and transmission coefficients for plane longitudinal incident waves: Geophysical Prospecting, 10, 304-351.

Nazar, B., 1991, An interpretative study of multicomponent seismic data from the Carrot Creek area of west-central Alberta, M. Sc. Thesis, The university of Calgary, Calgary, Alberta.

Shuey, R.T., 1985, A simplification of the Zoepritz equations: Geophysics, 50, p. 609-614.

Smith, G.C., and Gidlow, P.M., 1987, Weighted stacking for rock property estimation and detection of gas: Geophysical Prospecting, 35, 993-1014.

Xu, Y. and Bancroft, J.C., Joint AVO analysis of PP and PS seismic data: CREWES Research Report, 1997, Chapter 34.

ACKNOWLEDEGMENTS

Thanks to PDVSA-EP and PDVSA-Intevep for their support and permission to publish this work.

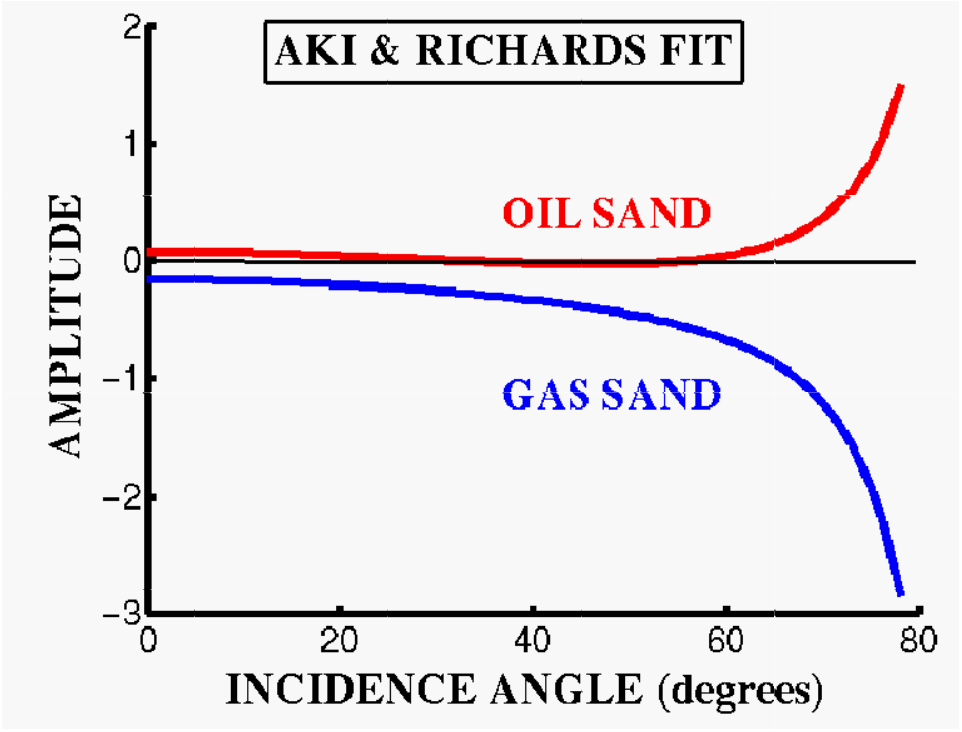

(a)

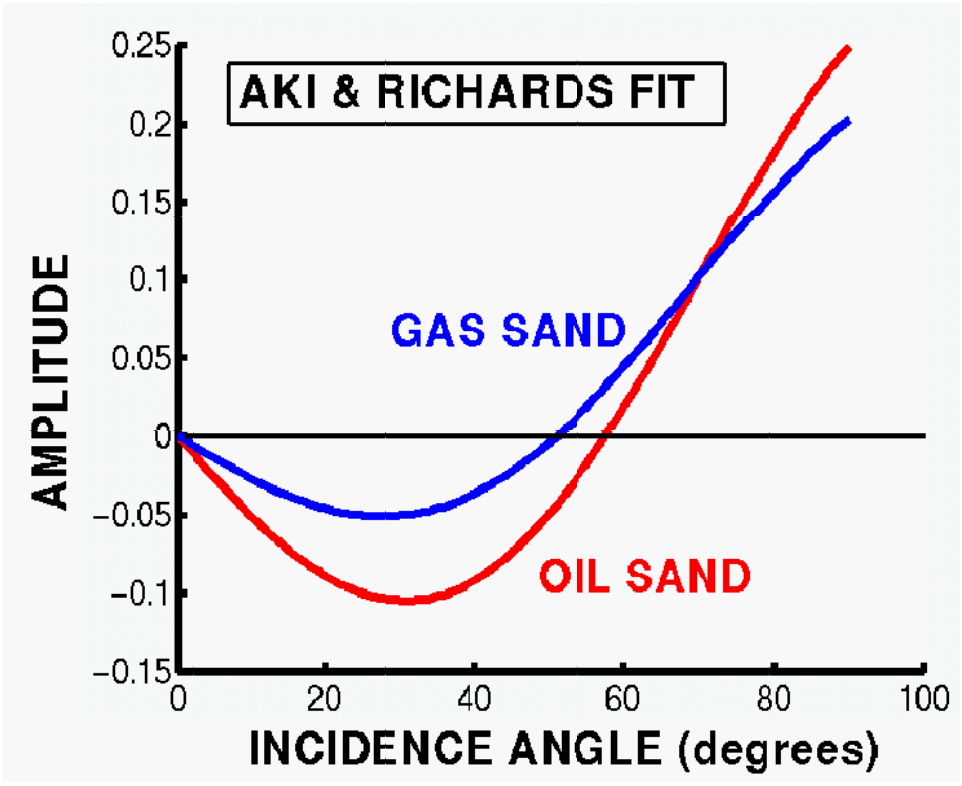

(b)

Figure 1. (a) R_{pp} vs incidence angle using Aki and Richards approximations for P-P data, (b) R_{ps} vs incidence angle using Aki and Richards approximations for P-S data. For the oil sand model we considered ρ_1 = 2.36 g/cc, ρ_2 = 2.27 g/cc, V_{p1} = 3170m/s, V_{p2} = 3734m/s, and V_{s1} = 1668m/s, V_{s2} = 2280m/s, while in the gas sand case we have ρ_1 = 2.40, ρ_2 = 2.14 V_{p1} = 3048, V_{p2} = 2440, and V_{s1} = 1245, V_{s2} = 1630.

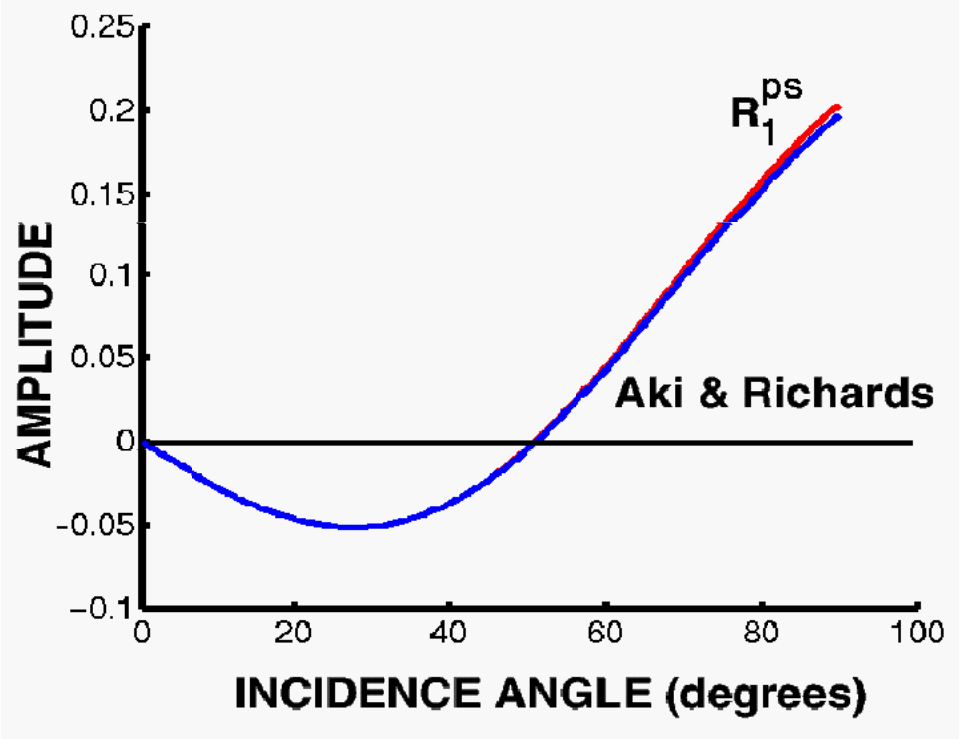

Figure 2. R_1ps versus Aki and Richards approximations.

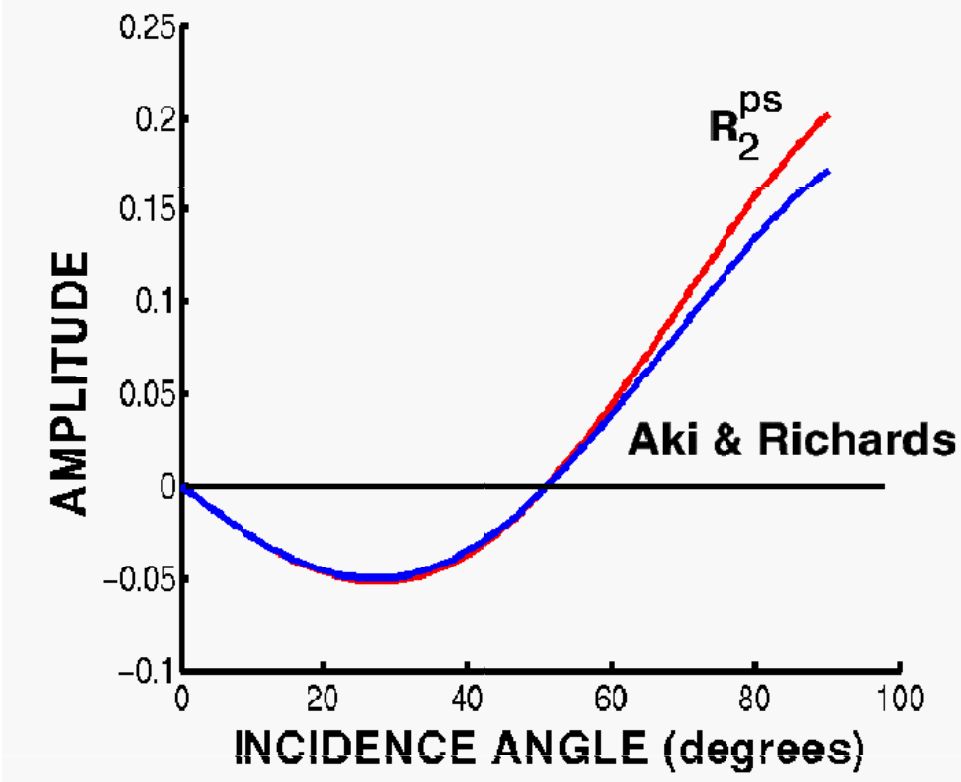

Figure 3. R_2^{ps} versus Aki and Richards approximations.

Contents

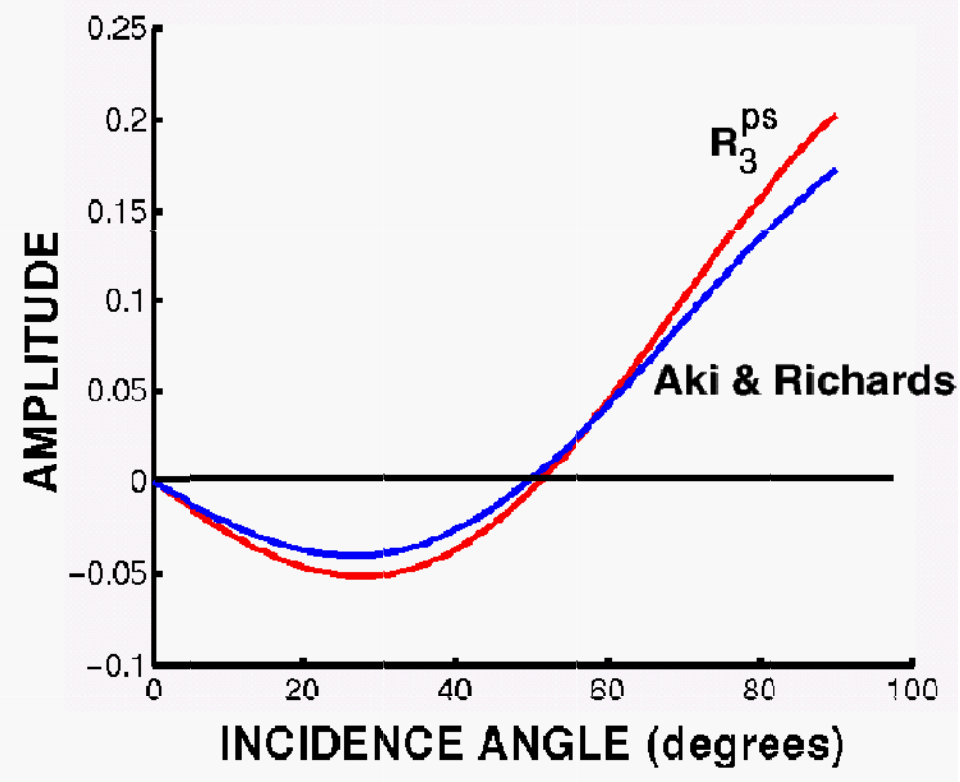

Figure 4. R_3^{ps} versus Aki and Richards approximations.

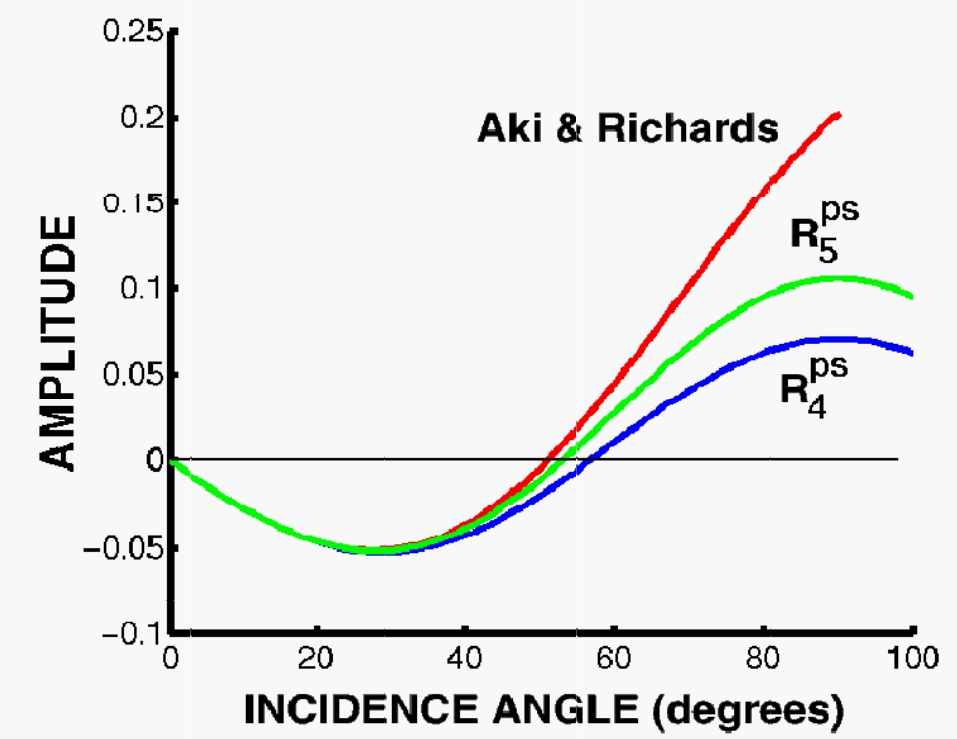

Figure 5. R_5^{ps} and R_6^{ps} versus Aki and Richards approximations.

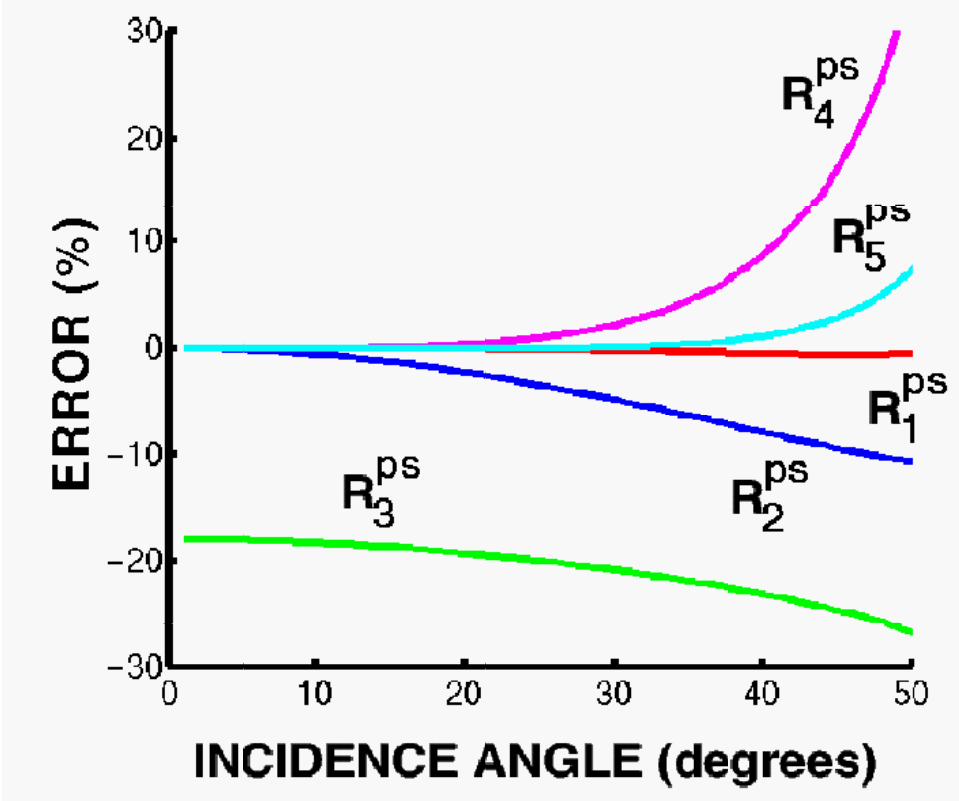

Figure 6. R^{ps} – Aki and Richards approximation error curves.

Contents